Supporting Information

Facile Synthesis of CNT Interconnected PVP-ZIF-8 Derived Hierarchical Porous Zn/N Co-doped Carbon Frameworks for Oxygen Reduction

Gourav Singla,‡[a] Siddheshwar N. Bhange, ‡[ab] Mani Mahajan[c] and Sreekumar Kurungot *[ab]

[a] Physical and Materials Chemistry Division, CSIR-National Chemical Laboratory, Pune, Maharashtra 411008, India.

[b] Academy of Scientific and Innovative Research (AcSIR), Ghaziabad-201002, India.

[c] Department of Physics and Centre for Energy Science, Indian Institute of Science Education and Research Pune, Pune, 411008, India

Email: k.sreekumar@ncl.res.in

‡ These authors contributed equally in this work

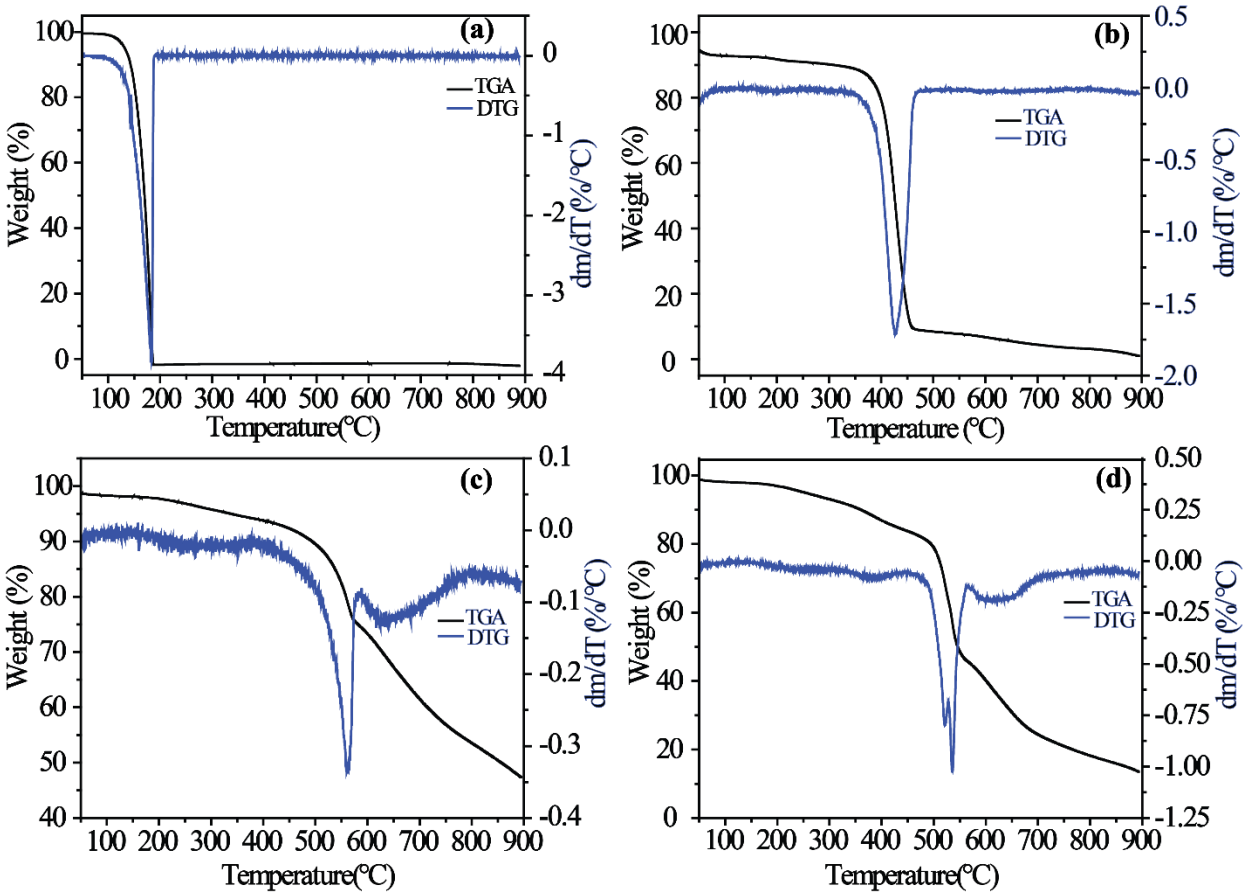

Fig. S1 TGA and the corresponding derivative TG (DTG) curves of (a) MIM, (b) PVP, (c) ZIF-8@CNT, and (d) PVP-ZIF-8@CNT measured in N_2 atmosphere.

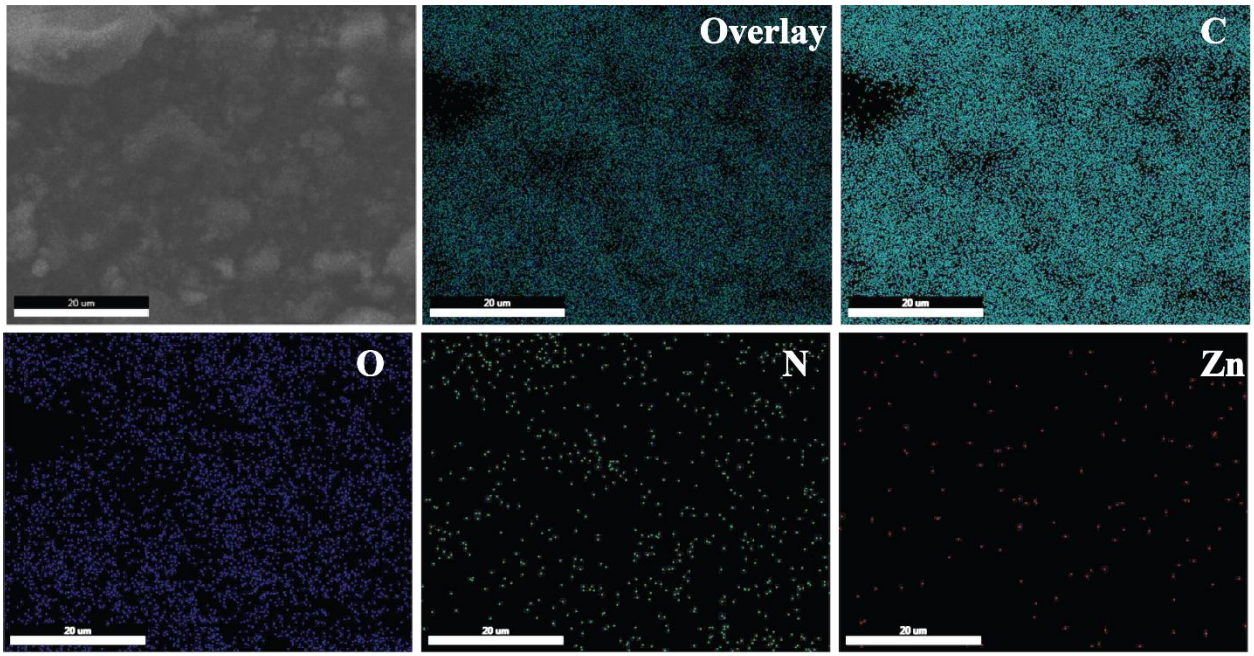

Fig. S2 Elemental mapping images of C, O, N and Zn of PVP-ZIF-8@CNT-900.

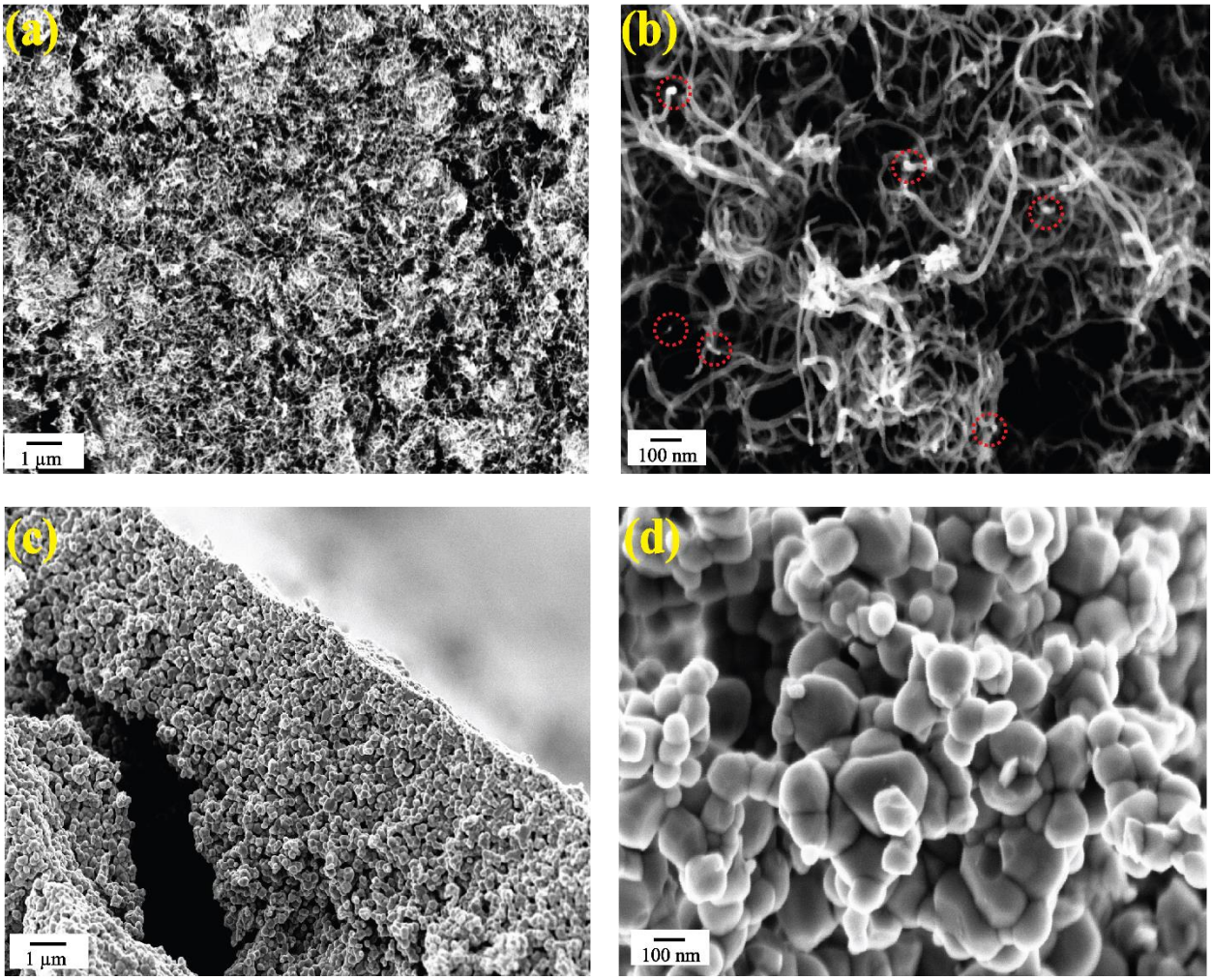

Fig. S3 SEM images of (a, b) ZIF-8@CNT-900 and (c, d) PVP-ZIF-8-900.

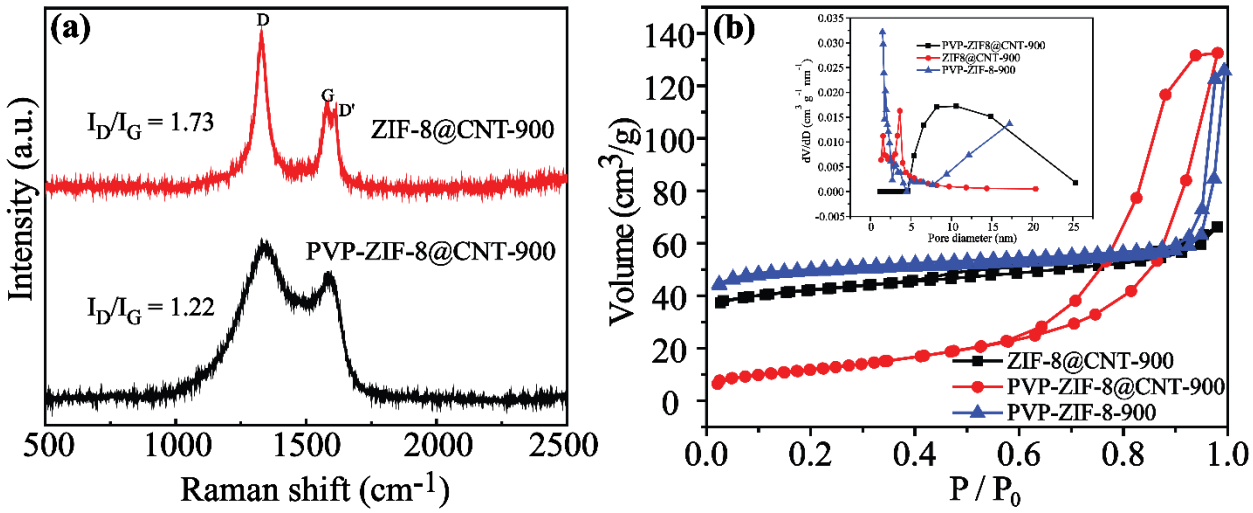

Fig. S4 (a) Raman spectra and (b) N_2 adsorption/desorption profiles of PVP-ZIF-8@CNT-900, ZIF-8@CNT-900 and PVP-ZIF-8-900 (Inset: BJH pore size distribution curves of PVP-ZIF-8@CNT-900, ZIF-8@CNT-900 and PVP-ZIF-8-900).

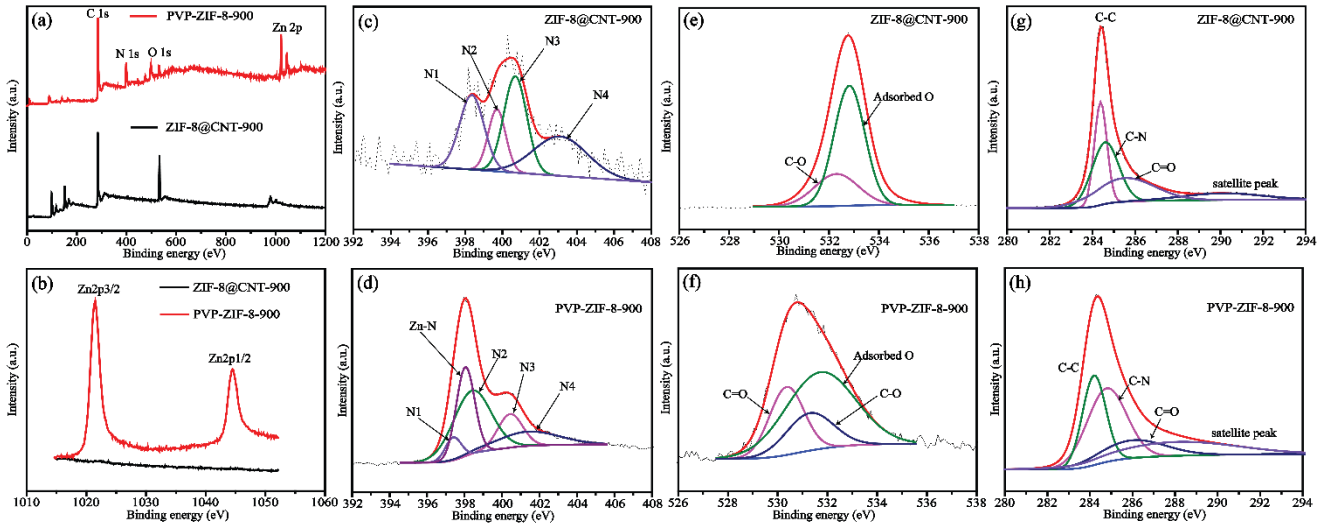

Fig. S5 (a) XPS survey spectra and (b) XPS spectra of Zn 2p for PVP-ZIF-8-900 and ZIF-8@CNT-900 samples; (c-h) deconvoluted XPS spectra of N 1s, O 1s and C 1s for ZIF-8@CNT-900 and PVP-ZIF-8-900.

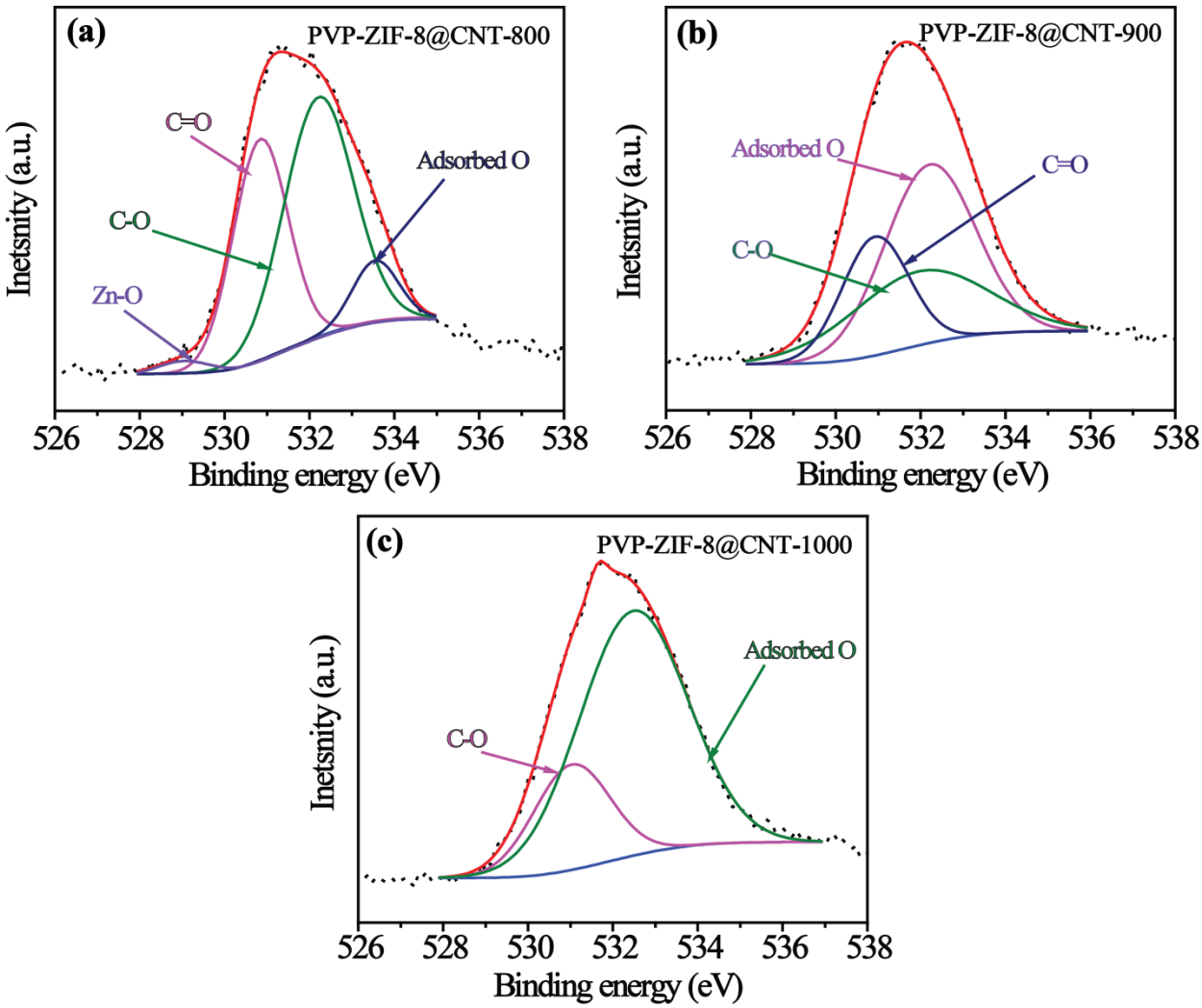

Fig. S6 XPS high-resolution spectra of O 1s for (a) PVP-ZIF-8@CNT-800, (b) PVP-ZIF-8@CNT-900 and (c) PVP-ZIF-8@CNT-1000.

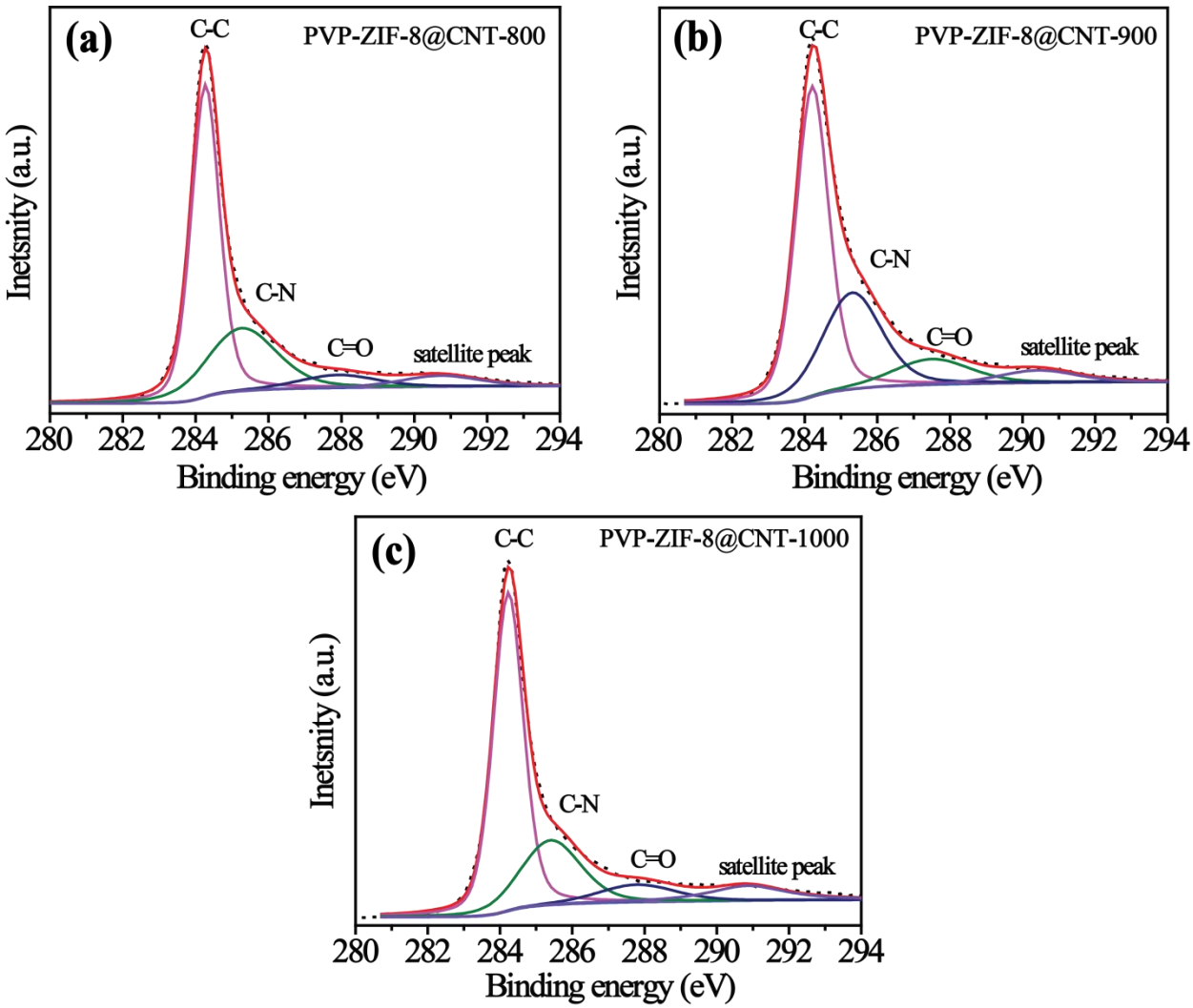

Fig. S7 XPS high-resolution spectra of C1s for (a) PVP-ZIF-8@CNT-800, (b) PVP-ZIF-8@CNT-900 and (c) PVP-ZIF-8@CNT-1000.

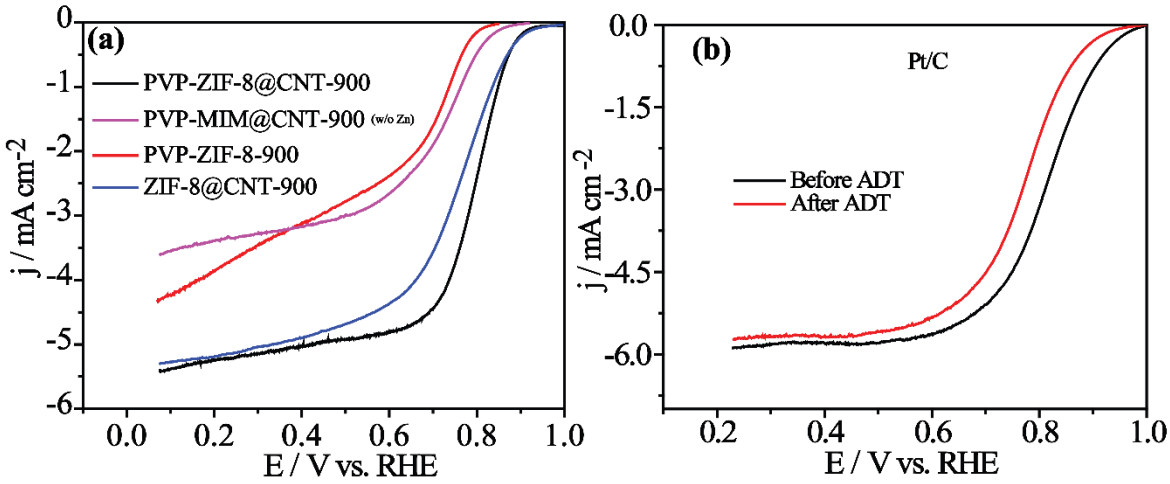

Fig. S8 (a) LSV profiles of the PVP-ZIF-8@CNT-900, PVP-MIM@CNT-900 (w/o Zn), PVP-ZIF-8-900 and ZIF-8@CNT-900 on a RDE electrode in O_2-saturated 0.1 M KOH solution at a rotation rate of 1600 rpm and a scan rate of 10 mV s^{-1}; (b) the RDE polarization curves of Pt/C in O_2-saturated 0.1 M KOH solution before ADT and after the 5000 potential cycles with the electrode rotation speed of 1600 rpm and scan rate of 10 mV s^{-1}.

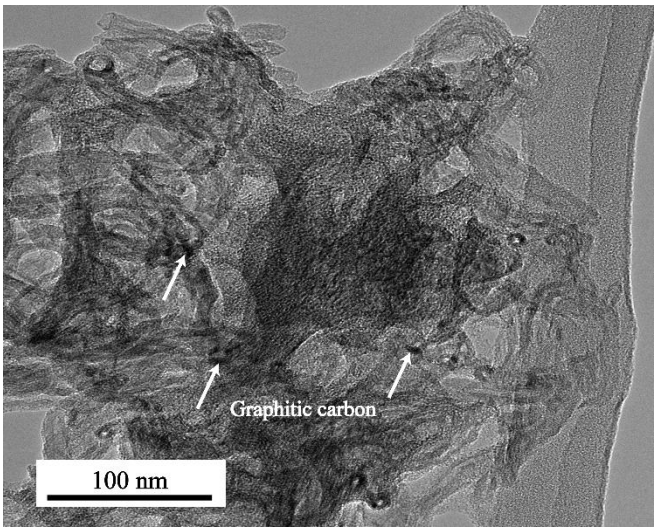

Fig. S9 TEM image of PVP-ZIF-8@CNT-900 after 5000 ADT cyclings.

Table S1. Elemental composition of PVP-ZIF-8@CNT-900, PVP-ZIF-8-900 and ZIF-8@CNT-900.

Sample		Zn	N	C	O
PVP-ZIF-8@CNT-900	MP-AES	4 wt.%	-	-	-
	XPS	7.3 wt.%	8.7 wt.%	73.7 wt.%	10.3 wt.%
PVP-ZIF-8-900	MP-AES	10 wt.%	-	-	-
	XPS	16.1 wt.%	15.8 wt.%	62.8 wt.%	5.3 wt.%
ZIF-8@CNT-900	MP-AES	-	-	-	-
	XPS	-	1.8 wt.%	75.6 wt.%	22.6 wt.%

Table S2. Nitrogen content and its types of coordination in PVP-ZIF-8@CNT-800, PVP-ZIF-8@CNT-900, PVP-ZIF-8@CNT-1000, ZIF-8@CNT-900 and PVP-ZIF-8-900.

Sample	Total N [at. %]	Pyridinic N [at.%]	Pyrrolic N [at.%]	Graphitic N [at.%]	Oxidized N [at.%]
PVP-ZIF-8@CNT-800	1.54	0.11	1.40	0	0.03
PVP-ZIF-8@CNT-900	8.3	1.32	3.82	2.95	0.21
PVP-ZIF-8@CNT-1000	2.74	0.64	0.32	1.44	0.34
ZIF-8@CNT-900	1.51	0.39	0.22	0.46	0.44
PVP-ZIF-8-900	15.8	1.29	8.42	2.92	3.17

Table S3. Oxygen reduction peak potential, onset potential and $E_{1/2}$ values recorded for all the catalysts in alkaline condition.

Sample	Oxygen reduction peak potential (V) vs. RHE	Onset potential (V) vs. RHE	$E_{1/2}$ (V) vs. RHE
PVP-ZIF-8@CNT-800	0.72	0.88	0.705
PVP-ZIF-8@CNT-900	0.78	0.96	0.795
PVP-ZIF-8@CNT-1000	0.75	0.93	0.770

Table S4. Comparison of the ORR performance of PVP-ZIF-8@CNT-900 with the other reported catalysts in 0.1 M KOH solution.

Catalyst	Loading (mg cm^{-2})	E_{onset} (V) vs RHE	$E_{1/2}$ (V) vs RHE	References
PVP-ZIF-8@CNT-900	**0.25**	**0.960**	**0.795**	**This study**
Co_3O_4@C-MWCNTs	0.33	0.890	0.810	S1
Co@Co_3O_4/NC	0.21	N/A	0.800	S2
N-Co_9S_8/G	0.20	0.941	0.770	S3
Co@N-C	0.20	N/A	0.820	S4
Co-MOF@CNT	0.21	0.910	0.820	S5
$Ni_xCo_yO_4$/Co–NG	0.20	N/A	0.804	S6
Cu-N/C	0.25	0.914	0.813	S7
N-doped Fe/Fe_3C@C	0.70	0.910	0.830	S8
LDH@ZIF-67-800	0.20	0.940	0.830	S9
GNC-Co	0.40	0.840	0.730	S10
ZIF8-Te-1000	0.10	0.881	0.790	S11
CoO_x NPs/BNG	N/A	0.950	0.805	S12
CoMn/pNGr	0.25	0.940	0.791	S13

Table S5: Comparison of the AEMFC performance for PVP-ZIF-8@CNT-900 with the other reported catalysts.

Catalyst	Loading (mg cm^{-2})	Membrane	Temperature (^{0}C)	P_{max} (mW cm^2)	References
PVP-ZIF-8@CNT-900	**2.0**	**Fuma-Tech FAA**	**60**	**45**	**This study**
40 wt% Ag/CNT	0.5	Fuma-Tech FAA	RT	26.1	S14
$CoFeN_x$/C	2.5	Tokuyama A-201	60	37	S15
Fe/Co-NpGr	2.5	Fuma-Tech FAA	50	35	S16
N-S/Gr- 1000	2.0	Fumapem FAA	RT	19.8	S17
FeNCNH	4.0	Fumapem FAA	50	35	S18
N-S-MPC	3.0	Tokuyama A-201	RT	21.7	S19
CoPC/C	3.0	Tokuyama A-901	RT	12.6	S20

References:

S1. X. Li, Y. Fang, X. Lin, M. Tian, X. An, Y. Fu, R. Li, J. Jin and J. Ma, *J. Mater. Chem. A*, 2015, **3**, 17392-17402.

S2. A. Aijaz, J. Masa, C. Rösler, W. Xia, P. Weide, A. J. R. Botz, R. A. Fischer, W. Schuhmann and M. Muhler, *Angew. Chem. Int. Ed.*, 2016, **55**, 4087-4091

S3. S. Dou, L. Tao, J. Huo, S. Wang and L. Dai, *Energy Environ. Sci.*, 2016, **9**, 1320-1326.

S4. M. Zhang, Q. Dai, H. Zheng, M. Chen and L. Dai, *Adv. Mater.*, 2018, **30**, 1705431.

S5. Y. Fang, X. Li, F. Li, X. Lin, M. Tian, X. Long, X. An, Y. Fu, J. Jin, J. Ma, *J. Power Sources*, 2016, **326**, 50-59.

S6. Y. Hao, Y. Xu, J. Liu and X. Sun, *J. Mater. Chem. A*, 2017, **5**, 5594-5600.

S7. Q. Lai, J. Zhu, Y. Zhao, Y. Liang, J. He, J. Chen, *Small*, 2017, **13**, 1700740.

S8. Y. Hou, T. Huang, Z. Wen, S. Mao, S. Cui, J. Chen, *Adv. Energy Mater.*, 2014, **4**, 1400337.

S9. Z. Li, M. Shao, L. Zhou, R. Zhang, C. Zhang, M. Wei, D. G. Evans, X. Duan, *Adv. Mater.*, 2016, **28**, 2337-2344.

S10. S. Li, D. Wu, C. Cheng, J. Wang, F. Zhang, Y. Su, X. Feng, *Angew. Chem. Int. Ed.*, 2013, **52**, 12105

S11. W. Zhang, Z. -Y. Wu, H. -L. Jiang and S. -H. Yu, *J. Am. Chem. Soc.*, 2014, **136**, 14385-14388.

S12. Y. Tong, P. Chen, T. Zhou, K. Xu, W. Chu, C. Wu and Y. Xie, *Angew. Chem. Int. Ed.*, 2017, **56**, 7121-7125.

S13. S. K. Singh, V. Kashyap, N. Manna, S. N. Bhange, R. Soni, R. Boukherroub, S. Szunerits and S. Kurungot, *ACS Catal.*, 2017, **7**, 6700-6710.

S14. A. Fazil and R. Chetty, *Electroanalysis*, 2014, **26**, 2380-2387.

S15. R. Z. Jiang and D. Chu, *J. Power Sources*, 2014, **245**, 352-361.

S16. T. Palaniselvam, V. Kashyap, S. N. Bhange, J. B. Baek and S. Kurungot, *Adv. Funct. Mater.*, 2016, **26**, 2150-2162.

S17. A. Arunchander, S. G. Peera, S. K. Panda, S. Chellammal and A. K. Sahu, *Carbon*, 2017, **118**, 531-544.

S18. S. M. Unni, S. Ramadas, R. Illathvalappil, S. N. Bhange and S. Kurungot, *J. Mater. Chem. A*, 2015, **3**, 4361-4367.

S19. N. N. Xu, T. S. Zhu, J. L. Qiao, F. Y. Zhang and Z. W. Chen, *Int. J. Hydrog. Energy*, 2016, **41**, 9159-9166.

S20. T. Zhu, X. Qing, P. Xu, Y. Song and J. Qiao, *ECS Transactions*, 2015, **66**, 105-110.